PERFORMANCE OF A HIGH VOLUME PM2.5 SAMPLER

A Thesis

by

HUAN LI

Submitted to the Office of Graduate Studies and Professional Studies of
Texas A&M University
in partial fulfillment of the requirements for the degree of

MASTER OF SCIENCE

Chair of Committee,	William B. Faulkner
Committee Members,	Calvin B. Parnell, Jr.
	John S. Haglund
Head of Department,	Steve Searcy

December 2013

Major Subject: Biological and Agricultural Engineering

ABSTRACT

Particulate matter (PM) is a complex mixture of extremely small particles suspended in the air. $PM_{2.5}$ is the fraction of particles suspended in the air with diameters that are nominally 2.5 μm and smaller. For regulatory purposes, $PM_{2.5}$ concentrations can be measured by a Federal Equivalent Method (FEM) sampler. Environmental Protection Agency (EPA) designates $PM_{2.5}$ samplers which meet the requirements specified in 40 Code of Federal Regulation (CFR), Part 53, Subpart F as FEM samplers.

Wind tunnels used to evaluate $PM_{2.5}$ samplers must satisfy the performance requirements for wind velocity uniformity and aerosol concentration uniformity. For wind velocity uniformity, mean wind speeds in the test section were within ±10 percent of the target (2 and 24 km/hr wind speeds), and the variation at any test point in the test section did not exceed 10% of the measured mean. For concentration uniformity, the coefficient of variation of the concentration was lower than 10% at 2 and 24 km/hr wind speeds.

The $PM_{2.5}$ sampler and two isokinetic samplers were placed into the wind tunnel and challenged with ammonium fluorescein solid particles with diameter from 1.5 μm to 4 μm at wind speed of 2 and 24 km/hr. The sampling effectiveness for each particle size can be obtained by fluorometric analysis. Based on the results of full wind tunnel tests and particle distribution data for aerodynamic particle sizer, a preliminary sampling effectiveness curve was determined by fitting a lognormal curve to the observed solid aerosol sampling effectiveness data by minimizing the sum of squared error between the predicted effectiveness and the data from full wind tunnel tests.

The cutpoints for 2 and 24 km/hr wind speed were 3.08 μm and 3.29 μm, respectively, out of the range of 2.5±0.2 μm, and mass concentration ratios (Rc) were larger than 1.05 except for the idealized fine aerosol size distribution. Therefore, the candidate sampler did not pass the full wind tunnel test.

The possible reason that the high volume $PM_{2.5}$ sampler failed to pass full wind test was the velocity inside the nozzle was lower than necessary to separate large particles from the sample flow.

ACKNOWLEDGEMENTS

I would like to thank my committee chair, Dr. Faulkner, for his trust throughout my M.S. study. I would also like to thank my committee members, Dr. Parnell and Dr. Haglund for their guidance and support.

Thanks to Dr. Karthikeyan and Dr. Lacey for letting me use the microscope and analysis software, making it much easier to measure diameters of tiny particles.

Thanks to Matthew Shimek for the hard work in the wind tunnel project. To Raleigh Smith, thank you for teaching me how to run whole tests and answering all questions.

To Chao Wang, Kai An, Thanks for being supportive of me through the tough times in College Station.

Finally, I want to say thanks to my parents for their understanding and supporting.

TABLE OF CONTENTS

Page

LIST OF FIGURES

Page

LIST OF TABLES

Page

CHAPTER I

INTRODUCTION

Particulate matter, also known as particle pollution or PM, is a complex mixture of extremely small solid particles and liquid droplets suspended in the air. $PM_{2.5}$ (Figure 1) is the fraction of particles suspended in the air with aerodynamic diameters that are nominally 2.5 μm and smaller. Aerodynamic diameter is the diameter of the spherical particle with a density of 1000 kg/m^3 that has the same settling velocity as the particle (Hinds, 2012). Particulate matter can be categorized as primary aerosols and secondary aerosols. Primary aerosols are emitted directly from sources to the atmosphere. Secondary aerosols are formed during atmospheric gaseous reactions from chemicals released from multiple sources, including power plants, automobile emissions and source of ammonia, among others (McMurry et al., 2004).

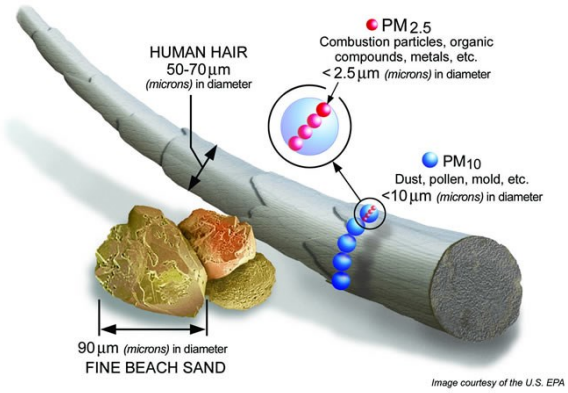

Figure 1. Comparison of $PM_{2.5}$ and human hair (USEPA, 2013b)

$PM_{2.5}$ effects on human health

Exposure to pollutants such as airborne particulate matter has been associated with increases in mortality and hospital admissions due to respiratory and cardiovascular disease. These effects have been found in short-term and long-term studies (Brunekreef and Holgate, 2002). Exposure to fine particulate has been associated with all-cause, lung cancer, and cardiopulmonary mortality. Each 10μg/m^3 elevation in fine particulate air pollution was associated with approximately a 4%, 6%, and 8% increased risk of all-cause, cardiopulmonary, and lung cancer mortality, respectively (Pope III et al., 2002).

In order to protect the public from adverse effects of air pollution, the Clean Air Act was enacted by the United States Congress in 1970.

Under the Clean Air Act, the Environmental Protection Agency (EPA) is required to set National Ambient Air Quality Standards (NAAQS) for pollutants considered harmful to public health and welfare. The current NAAQS for PM2.5 includes three standards (Table 1).

Table 1. National Ambient Air Quality Standards For PM2.5 (USEPA, 2013a).

Standard	Averaging Time	Level (μg/m^3)	Form
primary	Annual	12	annual mean, averaged over 3 years
secondary	Annual	15	annual mean, averaged over 3 years
primary and secondary	24-hour	35	98th percentile, averaged over 3 years

For regulatory purposes, $PM_{2.5}$ concentrations in the air can be measured by a Federal Reference Method (FRM) or Federal Equivalent Method (FEM) sampler. EPA

designates $PM_{2.5}$ samplers which meet the requirements specified in 40 Code of Federal Regulation (CFR), Part 53, Subpart F as FEM samplers. The tests required by Subpart F are shown in Table 2:

Table 2. Performance specifications for $PM_{2.5}$ Class II Equivalent samplers. (USEPA, 2013d).

Performance test	Specifications	Acceptance criteria
Full Wind Tunnel Evaluation	Solid Vibrating Orifice Aerosol Generator (VOAG) produced aerosol at 2 km/hr and 24 km/hr	Dp50[a]=2.5±0.2µm Numerical Analysis Results: 95% ≤ Rc[b]≤ 105%.
Wind Tunnel Inlet Aspiration Test	Liquid VOAG produced aerosol at 2 km/hr and 24 km/hr	Relative Aspiration: 95% ≤ A[c] ≤ 105%.
Static Fractionator Test	Evaluation of the fractionator under static conditions	Dp50= 2.5 µm ±0.2 µm Numerical Analysis Results: 95% ≤ Rc≤ 105%.
Loading Test	Loading of the clean candidate under laboratory conditions	Acceptance criteria as specified in the post-loading evaluation test.
Volatility Test	Polydisperse liquid aerosol produced by air nebulization of A.C.S. reagent grade glycerol, 99.5% minimum purity	Regression Parameters: Slope = 1 ±0.1, Intercept = 0 ±0.15 mg, r ≥ 0.97.

[a] Dp50 is cutpoint of sampler (i.e. the point of 50% sampling effectiveness)
[b] Rc = Mass concentration ratio between the candidate method and the reference method
[c] A = the ratio of the aerosol mass concentration measured by the candidate sampler to that measured by a reference method sampler.

The $PM_{2.5}$ concentration can be calculated as:

$$= \frac{m_{PM}}{Qt} \quad \textbf{(1)}$$

where

C = concentration of $PM_{2.5}$ ($\mu g/m^3$)

m_{PM} = mass of PM collected on a $PM_{2.5}$ sampler filter (μg)

Q = flow rate of the sampler (m^3/min), and

t = sampling period (min).

The flow rate for a FRM $PM_{2.5}$ sampler is 16.7 L/min (low volume $PM_{2.5}$ sampler) (40 CFR Part 50 Appendix L). For a typical sampling time (24 hours), the m_{PM} may be anywhere from 20 to 2000μg with most sample loads around 300μg (USEPA, 1998). Measuring the mass of particles collected requires a precise electronic balance with a readability and repeatability of at least of 1μg and a conditioning room capable of maintaining a mean temperature of 20 to 23°C, controlled to ±2°C, over a 24 hours period, and an average relative humidity (RH) of 30 to 40%, controlled to ±5% RH, over 24 hours (USEPA, 1998). The costs of these facilities are non-trivial and may prohibit implementation of $PM_{2.5}$ measurement.

To overcome the challenges associated with measuring low concentrations of $PM_{2.5}$, a high volume $PM_{2.5}$ sampler has been designed as a retrofit adaptation of existing high volume PM_{10} samplers (TE-6001 PM-10 sampler, Tisch Environmental Inc., Village of Cleves, OH). The adapter has a new plate that contains 40 nozzles designed to accelerate aspirated aerosols above the oil-wetted surface of an impactor well in order to collect particles nominally larger than $PM_{2.5}$ aerosols (Figure 2).

Figure 2. Retrofit nozzle bank with 40 nozzles in the sampler and single nozzle profile.

As shown in Figure 3, an aerosol is passed through a nozzle and the output stream directed towards a flat impaction plate. Particles with inertia exceeding a certain value are unable to follow the streamlines and collide with the surface of the impaction plate. Small particles can follow the streamlines and avoid hitting the plate. The parameter governing the collection efficiency of an impactor is the Stokes number (Hinds, 1999).

$$\boldsymbol{Stk = \frac{\tau U}{D_j/2} = \frac{\rho_p d_p^2 U C_c}{9\eta D_j}} \qquad \textbf{(2)}$$

where

τ = particle relaxation time (s)

U = gas velocity (m/s)

D_j = impactor jet diameter (m)

ρ_p = particle density (kg/m^3)

d_p = particle diameter (m)

C_c = Cunningham's correction factor (dimensionless), and

η = gas viscosity (Pa·s).

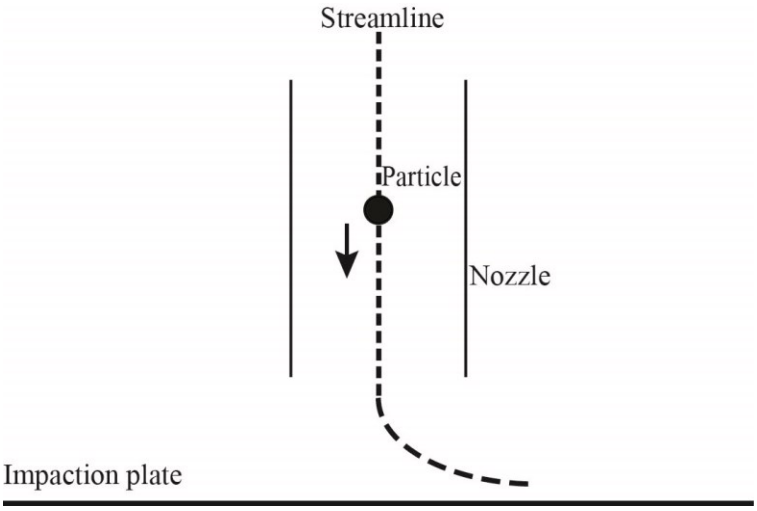

Figure 3. Cross-sectional schematic of an impactor.

If the impactor operates as intended, particle comprising the $PM_{2.5}$ fraction of an aerosol have sufficiently low Stokes numbers such that they are transmitted around the impactor and collected on a 0.203m×0.254m filter. The flow rate of the high volume $PM_{2.5}$ sampler is set at 40 CFM (1133L/min), 67.8 times higher than a FRM $PM_{2.5}$ sampler, allowing ~70 times more mass to be collected on the filter at a given concentration and sampling interval. With more mass collected during the same sampling period, the high volume $PM_{2.5}$ sampler can reduce the required resolution for electronic balances and decrease the sensitivity to filter conditioning and conditioning

room environments, therefore, reducing the cost of $PM_{2.5}$ measurement with no loss of precision in calculated concentrations.

Objective

The objective of this research was to evaluate the performance of a high volume $PM_{2.5}$ sampler under controlled conditions of a wind tunnel and propose any necessary design changes so that the sampler will achieve performance metrics of a Class II FEM $PM_{2.5}$ sampler as described in 40 CFR Part 53, Subpart F.

CHAPTER II

TEST SETUP FOR EVALUATING THE PM2.5 SAMPLER

To evaluate the performance of a $PM_{2.5}$ sampler, a wind tunnel is used to achieve conditions similar to typical ambient conditions. Wind tunnels used to evaluate $PM_{2.5}$ samplers must satisfy the performance requirements for wind velocity uniformity and aerosol concentration uniformity as stated in Table 3.

Table 3. EPA requirement for the performance of wind tunnel for PM2.5 sampler (USEPA, 2013d).

Parameter	PM2.5 Requirement
Wind speed	Mean wind speed is within ±10% for 2, 24 km/h
	Minimum of 12 test points
	Measuring techniques: precision≤ 2% ; accuracy ≤5%
Particle concentration	The COV is less than 10%
	5 or more evenly spaced isokinetic samplers Sampling zone: horizontal dimension > 1.2 times the width of the test sampler at its inlet opening vertical dimension > 25 cm

Wind tunnel

A wind tunnel was designed and fabricated at the Center for Agricultural Air Quality Engineering and Science (CAAQES) at Texas A&M University to achieve a uniform wind velocity and particle concentration as required. An overhead schematic of the wind tunnel is shown in Figure 4. The centrifugal fan (1) (PLR206, New York Blower Co., Willowbrook, IL) is equipped with a variable frequency drive to regulate

the speed of the fan. The wind tunnel body is located on an elevated platform to minimize vibration effects. The fan blows air through a vertical transmission duct which leads to a horizontal duct (2). A vibrating orifice aerosol generator (3) is located inside a mixing chamber (4). A Sterman disc (5) is used to induce mixing of the air and aerosol particles, which then pass through a flow straightener (6) in the 1 m × 1 m flow-stabilizing duct (7). At the end of this duct is the test chamber (8), which has an expanded cross sectional area to avoid wall effects and allow the base of the sampler to be located outside of the test area. Air exiting the test chamber passes through a 90º exhaust elbow (9) which directs the flow out through an exhaust fan (10) on the roof of the building.

Velocity uniformity

The velocity profile of the wind tunnel was measured using a hot wire anemometer (VelociCalc 8386, TSI, Inc., Shoreview, MN) with a precision of 0.01 m/s and an accuracy of ±1.5%. To obtain the velocity profile, the 1m x 1m cross sectional area used for sampling was divided evenly into a 4×4 grid, and the velocity was measured at the center of each grid as shown in Figure 5. The anemometer was set to sample at a rate of 1Hz for 15 seconds, and record the average wind speed across that time period. Twelve of these averages were taken at each point of the grid. Mean wind speeds in the test section were within ±10 percent of the target, and the variation at any test point in the test section did not exceed 10 percent of the measured mean, satisfying EPA's performance requirement for wind tunnels (Table 4).

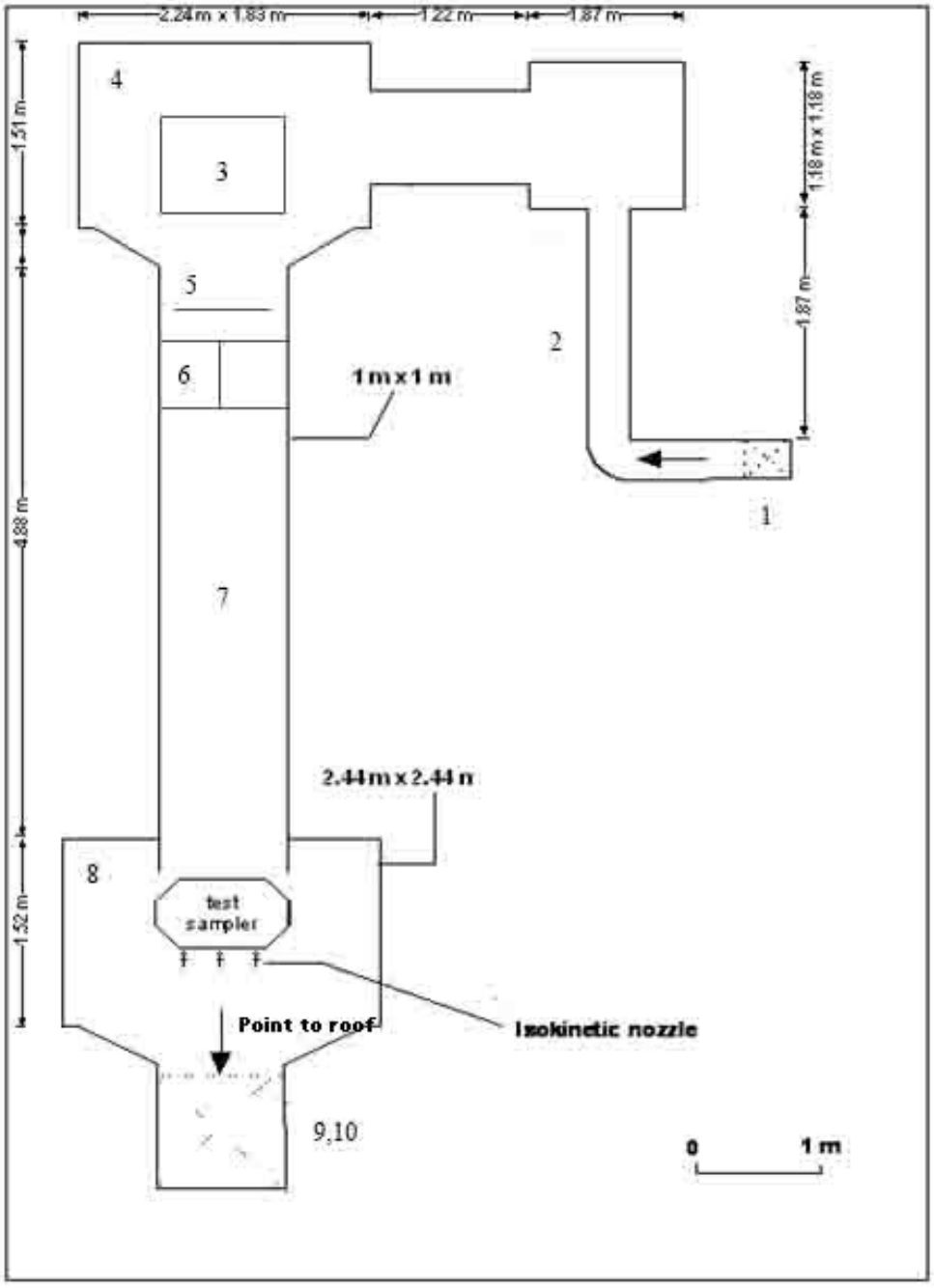

Figure 4. Schematic of wind tunnel used for high volume $PM_{2.5}$ sampler evaluation.

Table 4. Wind velocity uniformity of wind velocity.

Nominal Wind Speed(km/hr)	Mean Wind Speed (km/hr)	COV
2	1.92	1.8%
24	22.89	1.6%

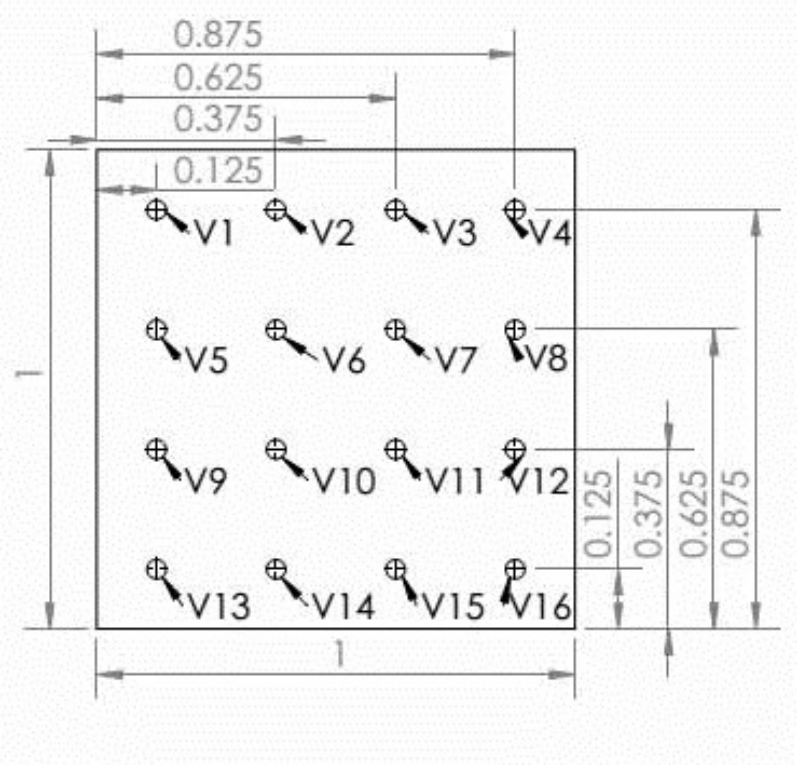

Figure 5. Positions of 16 test points for velocity uniformity measurements. (all dimensions in meters).

Concentration uniformity

A rack of nine isokinetic samplers was positioned in the test cross sectional area to measure the concentration uniformity of the wind tunnel. The 1m x 1m cross sectional area used for sampling was divided evenly into a 3×3 grid, and the particle concentrations were measured at the center of each grid (Figure 6). The probes used for

isokinetic samplers were machined conically from aluminum to hold 47 mm diameter filters. The inner surface of the nozzle was polished to reduce particle loss. The diameters of nozzles for 2 km/hr and 24 km/hr were 19.8mm and 10.2 mm, respectively. The flow rates of each sampler were 10.3 L/min at 2 km/hr wind speed and 32.4L/min at 24 km/hr wind speed.

For each wind speed, a VOAG was used to generate monodisperse solid ammonium fluorescein particles with aerodynamic diameters of 4μm in the wind tunnel. Particles were then collected for 1 hour at 2km/hr wind speed and 2 hours at 24km/hr wind speed, using polytetrafluoroethylene (PTFE) filters ($PM_{2.5}$ Air Monitoring Membrane, Whatman, Maidstone, United Kingdom) placed in the isokinetic samplers. Three replicate data points were collected at each sampling location for each wind speed.

Each of these nine filters were then removed from the isokinetic samplers and placed into 125mL jars (Nalgene, Penfield, New York). To each jar was added 15mL 0.01 mole/L ammonium hydroxide after the filter was placed into the jar. The jars soaked for a minimum of 4 hours before the solutions were analyzed with a fluorometer (Quantec model No. FM109515, Dubuque, Iowa). The fluorometer gave readings in Fluorescent Intensity Units (FIUs). An FIU is the uncalibrated output of the electrical signal conditioning circuit that processes the raw signal from the photomultiplier tube and is directly proportional to the concentration of the fluorescent tracer material.

Based on quality control parameters established by CAAQES personnel, a fluorometric signal is considered reliable when the FIU value of the test solution is at least twice the FIU value of the 0.01 mole/L ammonium hydroxide solvent. Test

durations varied from 1 to 2 hours to achieve a sufficient fluorometer reading. For 2 and 24 km/hr wind speeds, the COV of the concentration was lower than 10% (Table 5), satisfying EPA's performance requirements for the wind tunnel.

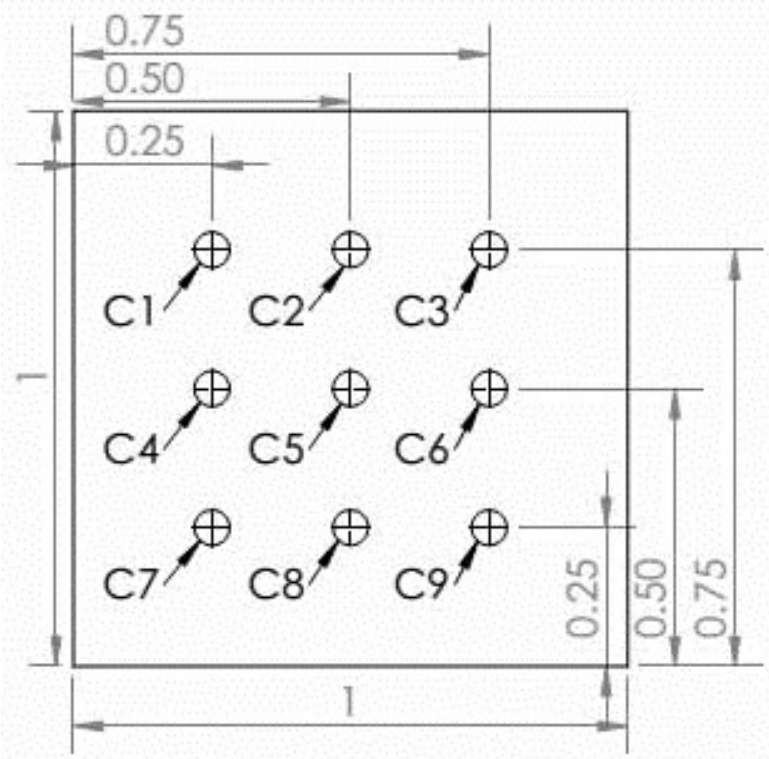

Figure 6. Positions of 9 test points for concentration uniformity measurements (all dimensions in meters).

Table 5. Concentration uniformity.

Nominal Wind Speed(km/hr)	COV of Concentration
2	9.7%
24	9.1%

Position of the two isokinetic samplers and candidate sampler

For testing under 40 CFR 53 Subpart F it is required that the blockage of samplers is no more than 15% of the test section area (40 CFR 53.62(c)(1)). In order to realize the 15% blockage, the sampler inlet would have to be placed 0.167m above the bottom of the sampling zone. Placement at this level would require sampling from an area outside the region in which concentration uniformity has been assessed. Faulkner (2013) requested a waiver of the blockage criteria and proposed placing the candidate sampler such that the leading edge is at point C8 (Figure 6). This placement would lead 20.3% blockage (18.5% by the candidate sampler, and 0.9% for each of isokinetic samplers). It was also proposed to measure concentrations of particles challenging the sampler by positioning isokinetic samplers at points C2 and C7, where normalized concentrations that are not significantly different than concentrations at point C8 were observed ($p<0.05$; Table 6). This waiver request was approved by EPA (Robert Vanderpool, personal communication, 01 March 2013).

Concentration measurements were normalized to allow comparisons between tests on a similar basis:

$$C_{norm,i,j} = \frac{C_{i,j}}{\left(\frac{\sum C_{i,j}}{n}\right)} \quad \textbf{(3)}$$

Where

$C_{norm,i,j}$ = normalized concentration for sampler "i" during test "j"

$C_{i,j}$ = concentration measured using sampler "i" during teste "j" ($FIU \cdot g \cdot L^{-1} \cdot min^{-1}$)

n = number of samplers (nine).

Table 6. Average normalized concentrations (± 95% confidence intervals; n = 3).

Sampling point	2 km/hr	24 km/hr
C1	1.05 ± 0.05	1.05 ± 0.01
C2	0.91 ± 0.04	0.96 ± 0.11
C3	1.18 ± 0.02	1.09 ± 0.05
C4	1.00 ± 0.03	0.97 ± 0.04
C5	0.86 ± 0.06	0.87 ± 0.03
C6	1.08 ± 0.04	1.05 ± 0.04
C7	0.93 ± 0.05	0.90 ± 0.09
C8	0.94 ± 0.07	0.91 ± 0.07
C9	1.05 ± 0.04	1.01 ± 0.06

Vibrating Orifice Aerosol Generator

A Vibrating Orifice Aerosol Generator (VOAG) (Figure 7) was used to generate the monodisperse particles with aerodynamic diameters specified in Table 7.

The components of the VOAG system include a HPLC pump (Model 12-6, Scientific Systems Inc., State College, PA), frequency generator (4003A, BK Precision, Yorba Linda, CA), aerosol particle generator (RNB Associaetes. Inc. Minneapolis, MN), and aerosol neutralizer (3054A, TSI Inc. Shoreview, MN).

A bottle of prepared liquid solution was pumped into the VOAG by a HPLC pump at a constant flow rate, forming a cylindrical liquid jet at the VOAG head. This jet was broken into equal size droplets by a vibrating orifice connected to the frequency generator. These droplets were then dispersed and diluted by dry air, forming monodisperse, dry, solid particles. After passing through the aerosol neutralizer, the

distribution of particles was measured using an Aerodynamic Particle Sizer (APS) (3321, TSI Inc. Shoreview, MN), and a small sample was collected onto a slide impactor. Monodisperse aerosols with desired size were then introduced into the wind tunnel, mixed with air, and used to challenge the candidate sampler.

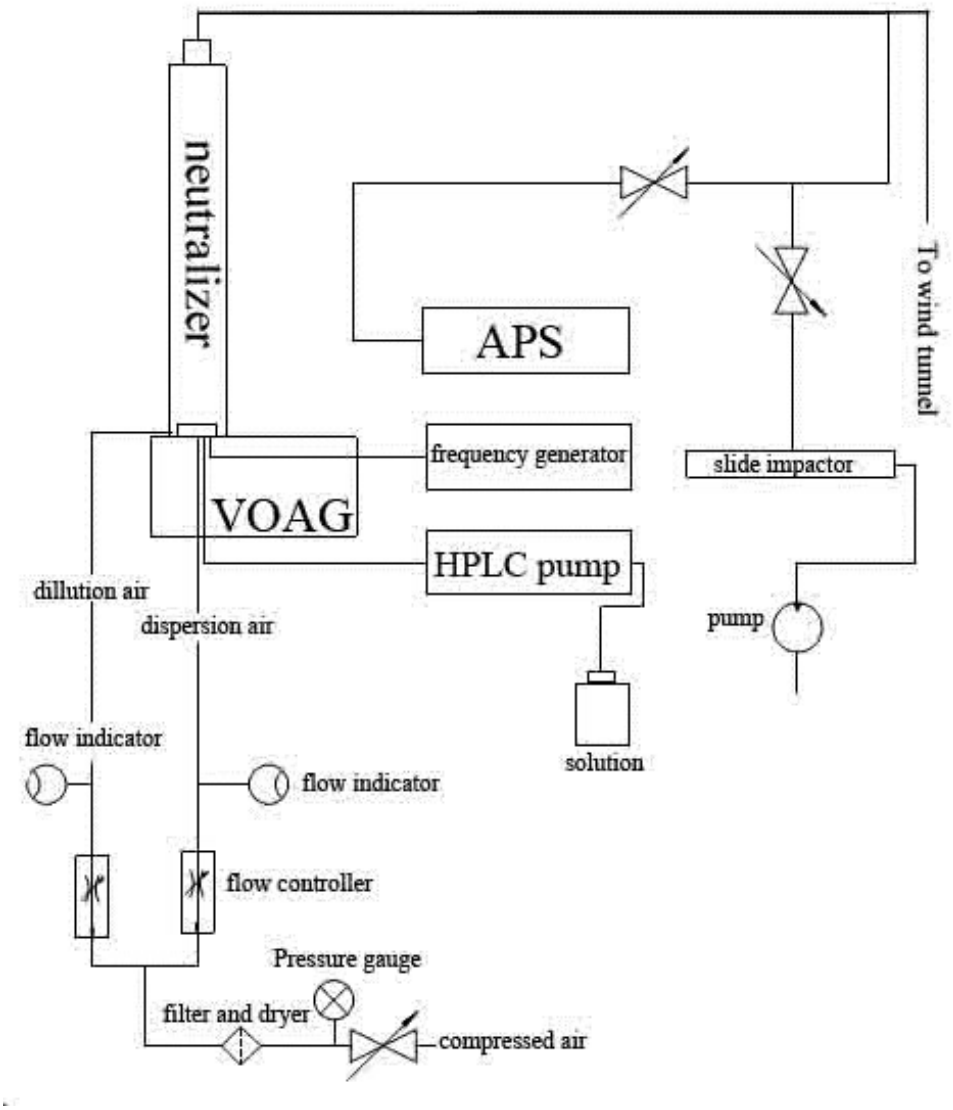

Figure 7. Schematic of VOAG system.

Table 7. Particle sizes for full wind tunnel test (USEPA, 2013d).

Nominal Mean Particle Size[a] (µm AD)
1.5±0.25
2.0±0.25
2.2±0.25
2.5±0.25
2.8±0.25
3.5±0.25
4.0±0.5

Liquid solutions used to generate aerosols are composed of a known mass of fluorescein (CAS 2321-07-05) dissolved in ammonium hydroxide (NH_4OH). When generated under proper conditions, the resulting particles are spherical and their aerodynamic diameter (AD) can be accurately calculated based on knowledge of the solution composition and the operational parameters of the VOAG (Berglund and Liu, 1973).

The chemical reaction which produces ammonium fluorescein involves the substitution of an ammonium cation (NH_4+) for a hydrogen anion (H+). In conjunction with the known density of ammonium fluorescein, the formula weights of the reactants were used to calculate the density of fluorescein:

$$\boldsymbol{\rho_{fl} = \rho_{af}\left(\frac{FW_{fl}}{FW_{fl}+FW_{NH4}-FW_{H}}\right)} \quad \textbf{(3)}$$

where

ρ_{fl} = density of fluorescein (g/cm^3)

ρ_{af} = density of ammonium fluorescein (g/cm^3)

FW_{fl} = formula weight of fluorescein = 332.31 g·mole^{-1}

FW_{NH4} = formula weight of ammonium cation = 18 g·mole^{-1}, and

FW_H = formula weight of hydrogen anion = 1 g·mole^{-1}.

The required mass of fluorescein was then calculated based on the volume of the final solution:

$$\boldsymbol{m_f = \rho_{fl} \cdot C \cdot V_c} \quad \textbf{(4)}$$

Where

m_f = mass of fluorescein (g)

C = volume concentration of the liquid solution (dimensionless), and

V_c = volume of the final solution (mL) (1000 mL).

The stoichiometric reactions between aqueous ammonia and fluorescein require equal molar quantities between the reactants. Excess ammonium hydroxide (three times quantities that required stoichiometrically) was added in the reactions to ensure all of fluorescein reacted to form ammonium fluorescein. Excess ammonium hydroxide would volatilize during particle formation, thereby not affecting the final size of the generated particles. Based on the desired concentration factor and the concentration of ammonium hydroxide used (14.5 mole/L or 68.97 ml/mole), the volume of concentrated ammonium hydroxide required was calculated:

$$\boldsymbol{V_{NH4OH} = \frac{m_f}{FW_{fl}} \cdot 68.97 \cdot F} \quad \textbf{(5)}$$

Where

V_{NH4OH}= volume of required concentrated ammonium hydroxide (mL)

m_f = mass of fluorescein (g)

FW_{fl} = formula weight of fluorescein ($g \cdot mole^{-1}$), and

F= factor for excess ammonium hydroxide = 3.

When generating solutions, the actual mass of fluorescein used in solution production sometimes differed slightly from the theoretical value calculated in eq 5, Therefore, the actual solution volumetric concentration was calculated:

$$\boldsymbol{C = \frac{m_f}{\rho_f V_c}} \quad \textbf{(6)}$$

Where

C = the actual solution volumetric concentration (dimensionless)

m_f = mass of fluorescein (g)

ρ_f = density of fluorescein (g/cm^3).and

V_c = volume of final solution (mL) = 1000 mL.

The volume of each droplet produced by the VOAG is the liquid flow rate divided by the vibrational frequency, so the physical particle diameter was calculated as:

$$\boldsymbol{Dp_p = \left(\frac{6Q_l C}{\pi f}\right)^{\frac{1}{3}}} \quad \textbf{(7)}$$

Where

Dp_p = physical particle diameter (μm)

Q = solution flow rate (mL/s) =0.093 mL/s

C = volumetric concentration of aerosol material in the solution (dimensionless)

f = VOAG frequency (Hz) =150000Hz (frequencies were adjusted during some tests, as needed, to minimize satellite droplets).

All generated particles were spherical, so their aerodynamic diameters were calculated as:

$$\boldsymbol{D_{p_a} = D_{p_p}\sqrt{\rho_p}} \quad \textbf{(8)}$$

Where

Dp_a = aerodynamic particle diameter (μm)

ρ_p = particle density (g/cm^3).

Based on equations 3-8, the mass of fluorescein and volume of ammonium hydroxide were calculated for each desired aerodynamic particle diameter (Table 7).

CHAPTER III

HIGH VOLUME SAMPLER PERFORMANCE EVALUATION

Introduction

The Tisch Environmental High Volume $PM_{2.5}$ sampler (TE-6001-2.5-I PM2.5 SSI, Tisch Environmental Inc., Village of Cleves, OH) is a retrofit to the Tisch Environmental High Volume FRM PM_{10} sampler. The aspiration characteristics of that sampler were well known. Therefore, the wind tunnel inlet aspiration test, static fractionator test, loading test, and volatility test were not required for Tisch Environmental High Volume $PM_{2.5}$ sampler (Robert Vanderpool, personal communication, 04 March 2013). Therefore, the tests described in this research focused on the full wind tunnel evaluation only.

For the full wind tunnel test, the effectiveness of the candidate sampler was evaluated at wind speeds of 2 and 24 km/hr for aerosols of the size specified in Table 7. Sampling effectiveness was calculated as the ratio of the mass concentration of particles of a specific size reaching the sampler filter to the mass concentration of particles of the same size approaching the sampler.

Method

The Tisch high volume $PM_{2.5}$ sampler was evaluated in the wind tunnel by the following procedure (USEPA, 2013c).

1. Generate aerosol.

A bottle of solid particle solution constructed to achieve the desired particle size was attached to the HPLC pump. The flow rate of the pump was set at 0.093 mL/min and the frequency generator was set at 150 kHz. After the VOAG system was filled with the solid particle solution, the valve of the VOAG was closed, forming a jet at the VOAG head. The aerosol neutralizer was installed on top of the VOAG head to discharge any static charge developed on the aerosol particles.

The aerosols generated by VOAG were then introduced into an APS to measure the particle sizes distribution. The frequency of frequency generator and flow rate of dilution and dispersion air were tuned to achieve a nominally monodisperse distribution with minimal satellites.

2. Verify the quality of the test aerosol.

For each aerosol test, a glass slide (frosted slides 48312-003, VWR International, Radnor, PA) was prepared with a coating of high vacuum silicon grease (high vacuum grease, Dow Corning, Midland, MI). This slide was then loaded into a glass slide impactor (Figure 8) described by Faulkner and Haglund (2012). The glass slide impactor was placed into the test chamber. The impactor drew particle-laden air at a flow rate of 17 L/min through a 6.35 mm diameter orifice, which was 3.7 mm from the slide surface. The solid ammonium fluorescein particles that impacted the slide were collected by the silicon grease coating. The particles collected on glass slide were then measured under a microscope (Eclipse TS100, Nikon Instruments Inc., Melville, NY). The populations of multiplets were analyzed by NIS-Elements Br Microscope Imaging Software (Nikon Instruments Inc., Melville, NY). If the population of multiplets exceeded 10%, VOAG

operating parameters were adjusted until this population of multiplets was lower than 10%.

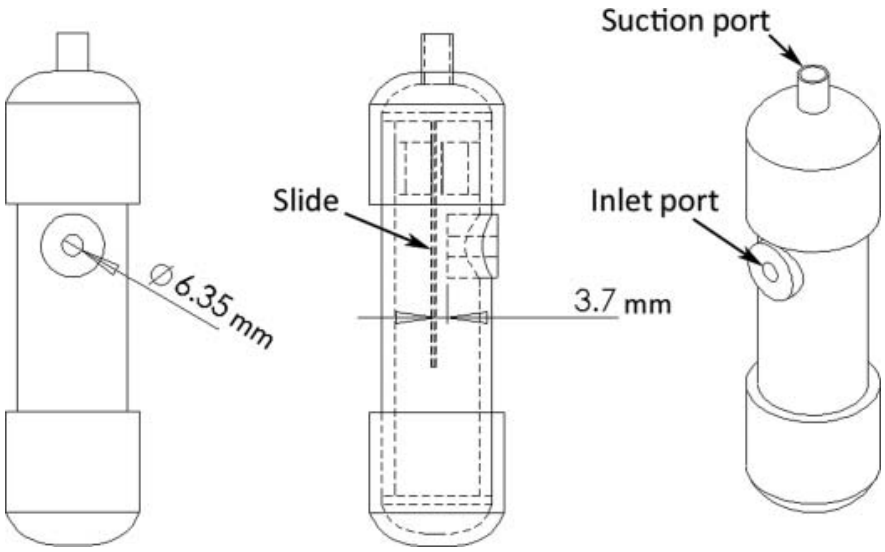

Figure 8. Slide impactor (Faulkner and Haglund, 2012).

3. Collect aerosols with the reference samplers and the candidate sampler.

The 90mm glass fiber filters (TCLP Glass Fiber Filters, Pall Life Sciences, Port Washington, NY) were loaded into two isokinetic samplers. The two isokinetic samplers were placed at points C2 and C5 (Figure 6). A 0.203m×0.254m glass fiber filter (EPM 2000 high-volume air sampling filter paper, Maidstone, United Kingdom) was loaded into the Tisch Environmental High Volume $PM_{2.5}$ sampler. The inlet of candidate sampler was placed at point C8 (Figure 6).

Two pumps (Model G608NGX, General Electric commercial motors, Fairfield, CT) were connected to the isokinetic samplers. The flow rates of the isokinetic samplers

were measured using two flow meters (D-AFC-09 flow meter, Hi-Q environmental products, San Diego, CA) and adjusted using two valves (SS-8BG, Swagelok, Solon, OH) to keep both of isokinetic samplers operating at sample flow rates of 114 L/min during the tests. The diameters of nozzles for 2 km/hr and 24 km/hr were 2.6 in. (66.0 mm) and 0.75 in. (19.1mm), respectively. The flow rate of candidate sampler was set to 40CFM (1133 L/min).

The sampling time was set to 30min for each test. After each test, the filters were removed from the samplers, and were then placed into 0.01 mole/L ammonium hydroxide for fluorometric analysis.

After a set of three tests were completed for a given particle size, the VOAG system was flushed with pure ethanol to avoid clogging and contamination of subsequent tests.

4. Calculations of sampling effectiveness.

The mass concentration of particles measured using each isokinetic sampler was calculated as:

$$\boldsymbol{C_{iso} = \frac{FIU_{iso} \cdot m_{L,iso}}{Q \cdot t}} \quad \textbf{(9)}$$

Where:

FIU_{iso} = average net fluorometric intensity of isokinetic sampler (FIU)

$m_{L,iso}$ = mass of liquid in which isokinetic filter was soaked (g)

Q = isokinetic sampler volumetric flow rate ($L \cdot min^{-1}$) and

t = sampling time (min)

The mass concentration of candidate sampler was calculated as:

$$C_{cand} = \frac{FIU_{cand} \cdot m_{L,cand}}{Q \cdot t} \quad (10)$$

Where:

FIU_{cand} = average net fluorometric intensity of candidate sampler (FIU)

$m_{L,cand}$ = mass of liquid in which candidate filter was soaked (g)

Q = candidate sampler volumetric flow rate ($L \cdot min^{-1}$); and

t = sampling time (min)

The sampling effectiveness of candidate sampler was calculated as:

$$E = \frac{C_{cand}}{(C_{iso,1}+C_{iso,2})/2} \times 100\% \quad (11)$$

The coefficient of variation (CV_E) for the replicate sampling effectiveness measurements of the test sampler was calculated as:

$$CV_E = \frac{Standard\ Deviation\ of\ E}{average\ of\ E} = \frac{\sqrt{\frac{\sum_{i=1}^{3} E_i^2 - \frac{1}{3}\left(\sum_{i=1}^{3} E_i\right)^2}{2}}}{(E_1+E_2+E_3)/3} \times 100\% \quad (12)$$

If the value of CV_E exceeded 10%, the test run (steps 1 to 4) was repeated until CV_E was lower than 10%.

CHAPTER IV

RESULTS AND CONCLUSIONS

Results of the full wind tunnel evaluation tests are shown in Table 8. A preliminary sampling effectiveness curve was determined by fitting a lognormal curve to the observed solid aerosol sampling effectiveness data by minimizing the sum of squared error (SSE) between the predicted effectiveness and the data shown in Table 8 without multiplet correction. Sampling effectiveness values of 100% and 0% for particle sizes of 1µm and 10µm, respectively, were added to the observed data per the requirements of 40 CFR Part 53.62(e)(1). Microsoft Excel® was used to fit the lognormal curve to the data by minimizing SSE between observed effectiveness values and the expected values (eq. 13).

Table 8. Full wind tunnel evaluation tests results.

	Wind speed of 2 km/hr			**Wind speed of 24 km/hr**		
Nominal size (µm)	**Calculated particle size (µm)**	**Observed Sampling Effectiveness[a]**	**CV_E[b]**	**Calculated particle size (µm)**	**Observed Sampling Effectiveness[a]**	**CV_E**
1.5	1.53	96.40%	16.8%	1.56	98.30%	6.6%
2	1.96	78.50%	4.0%	1.94	102.60%	13.6%
2.2	2.16	86.60%	5.7%	2.11	72.40%	3.3%
2.5	2.49	48.90%	3.8%	2.45	58.80%	6.7%
2.8	2.84	47.90%	4.3%	2.84	56.6%	7.0%
3.5	3.49	45.50%	6.7%	3.25	40.80%	6.7%
4	3.75	22.00%	4.6%	3.94	25.20%	46.0%

[a] Measured sampling effectiveness, not corrected for multiplets and satellites
[b] CV_E= coefficient of variation

The sum of squared error (SSE) was calculated as:

$$\boldsymbol{SSE = \sum(E_i - \eta_{ex,i})^2} \quad \textbf{(13)}$$

Where

E_i = measured sampling effectiveness for particle size i, and

$\eta_{ex,i}$ = expected (i.e., modeled) sampling effectiveness for particle size i.

Multiplet correction was then applied to sampling effectiveness data. For each nominal particle size shown in Table 8, measurements of particle size collected with the APS were used to quantify the relative mass concentrations of satellites and multiplets. A "particle size correction factor" (f) was calculated to correct APS-measured particle size data:

$$\boldsymbol{f = \frac{D_a}{D_{APS,VMD}}} \quad \textbf{(14)}$$

Where:

D_a = calculated aerodynamic diameter of "monodisperse" particles (μm)

$D_{APS,VMD}$ = volume mean diameter reported by the APS (μm).

This particle size correction factor was then applied to all APS-reported particle sizes for a given test. The expected sampling efficiency for each test aerosol was then calculated:

$$\boldsymbol{\eta_i = \int [\eta(d_p) \cdot f_{m,i}(d_p)]\, dd_p} \quad \textbf{(15)}$$

Where:

η_i = expected sampling efficiency for test aerosol i,

$\eta(d_p)$ = modeled sampling efficiency for particles of size d_p, and

$f_{m,i}(d_p)$ = relative mass frequency of particles of size d_p in test aerosol i.

The modeled sampling efficiency for particles of size d_p was calculated based on a lognormal sampling effectiveness curve (eq. 16):

$$\eta(d_p) = 1 - \frac{1}{ln(\sigma)\sqrt{2\pi}} exp\left(-\frac{\left(ln(d_p) - ln(\overline{d_p})\right)^2}{2(ln(\sigma))^2}\right) \quad \textbf{(16)}$$

Where:

σ = slope of sampling efficiency of sampler,

$\overline{d_p}$ = cutpoint of the sampler.

With the expected sampling efficiency for each test aerosol defined, the sampling efficiency model was fit to the experimental data by adjusting the slope and cutpoint of the sampler using Microsoft Excel® to minimize the SSE between observed effectiveness values and fitted curves (eq. 13). The cutpoint diameter at each wind speed was then determined from the corrected effectiveness curves (Table 9), and the two resultant penetration curves were then each numerically integrated with three idealized ambient particle size distributions to provide six estimates of measured mass concentration as specified in Subpart F (USEPA, 2013d).

Table 9. Cutpoint and expected mass concentration for various aerosol distributions at 2 and 24 km/hr wind speeds.

Wind Speed(km/hr)	Cutpoint (µm)	Mass concentration for aerosol size distributions (µg/m^3)		
		Coarse	"Typical" coarse	Fine
2	3.08	17.372[a]	37.072[b]	80.456[c]
24	3.29	17.782[d]	37.489[e]	81.662[f]
Ideal Sampler		13.814[a]	34.284[b]	78.539[c]

[a] Mass concentration calculations are shown in Appendix C
[b] Mass concentration calculations are shown in Appendix D
[c] Mass concentration calculations are shown in Appendix E

Table 9 continued
[d] Mass concentration calculations are shown in Appendix F
[e] Mass concentration calculations are shown in Appendix G
[f] Mass concentration calculations are shown in Appendix H

After establishing the multiplet corrected curves for each wind speed (Figure 9), the sampling efficiency at each particle size was determined, and the expected mass concentration that would be collected by the sampler when challenged with a given aerosol was calculated as:

$$\boldsymbol{C_{cand} = \int [\eta(d_p) \cdot C(d_p)] dd_p} \quad \textbf{(17)}$$

Where:

C_{cand} = expected mass concentration to be measured by the sampler ($\mu g/m^3$)

$\eta(d_p)$ = sampling efficiency for particles of size $d_{p,}$(μm)

$C(d_p)$ = mass concentration of particles of size d_p in various aerosol distributions described in Table F4-F6 of 40 CFR part 53 subpart F ($\mu g/m^3$).

Based on the expected mass concentrations for various aerosol distributions (Table 9) and ideal sampler mass concentration described in Table F3 of 40 CFR part 53 Subpart F, the mass concentration ratio (R_c) between the candidate method and the reference method were determined for each wind speed and particle size distribution (Table 10).

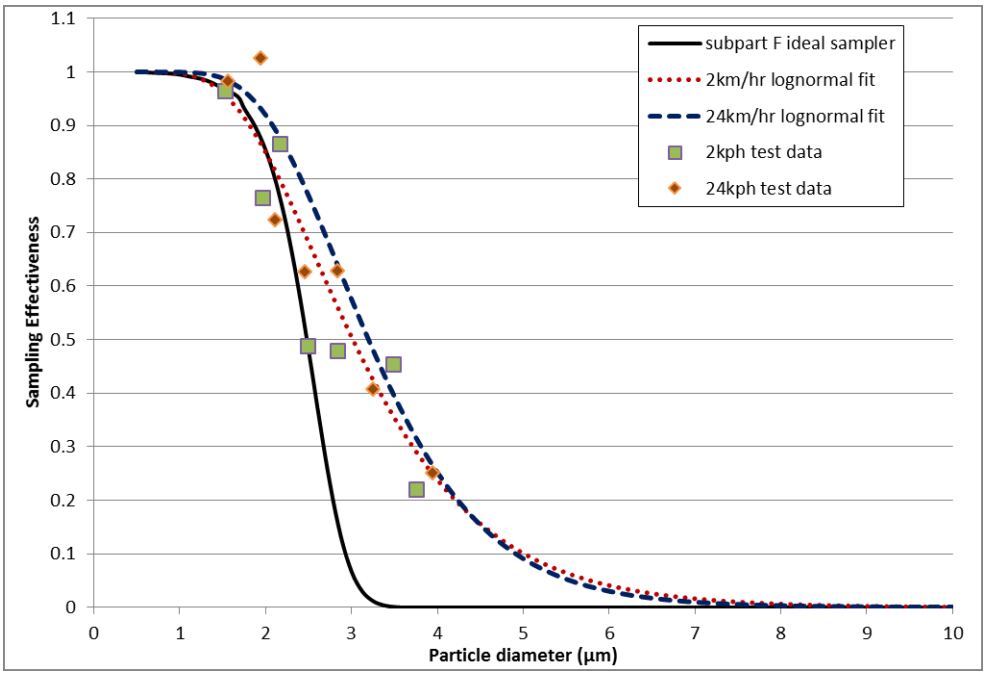

Figure 9. Multiplet-corrected sampling effectiveness curves at wind speeds of 2 and 24 km/hr.

Table 10. Mass concentration ratio between the candidate method and the reference method for 2 and 24 km/hr wind speed.

Wind Speed (km/hr)	Idealized coarse aerosol size distribution	Idealized "typical" coarse aerosol size distribution	Idealized fine aerosol size distribution
2	1.26	1.08	1.02
24	1.29	1.09	1.04

The cutpoints for 2 and 24 km/hr wind speed were out of the range of 2.5±0.2 µm, and mass concentration ratios (Rc) were larger than 1.05 except for the idealized fine aerosol size distribution. Therefore, the candidate sampler did not pass the full wind tunnel test.

The main reason the sampler did not pass the full wind tunnel test is the high sampling effectiveness observed at 2.8, 3.5 and 4μm particles, which were much higher than the ideal sampling efficiencies.

One possible reason for the high sampling effectiveness was that there was leaking between the nozzle rack and filter. Air leakage can effectively reduce the velocity through each of the nozzles for a given total flow rate. The reduced velocity would alter the particle Stokes number, thereby increasing the effectiveness of the sampler for all particle sizes.

In order to test whether leaking was the reason for high sampling effectiveness of large particles, a hard gasket that seal the chamber inside which the filter was placed was replaced by a soft one (Figure 10) that allowed for a better seal between sampler components, thereby reducing leakage. Table 11 shows the sampling effectiveness before and after replacing the gasket. It can be seen that the efficiencies stayed almost the same. Therefore, leaking was not the main cause for the high sampling effectiveness for large particles.

Figure 10. New gasket inside the sampler.

Table 11. Sampling effectiveness before and after replacing the gasket.

	Wind speed of 2km/hr		Wind speed of 24 km/hr	
	Particle size (µm)	**Sampling effectiveness**	**Particle size (µm)**	**Sampling effectiveness**
Hard gasket	2.8	49.2%	2.8	64.9%
	3.5	47.0%	3.5	42.5%
Soft gasket	2.8	58.5%	2.8	61.8%
	3.5	44.1%	3.5	41.0%

Another possible reason for the high sampling effectiveness of large particles was the velocity inside the nozzle was lower than necessary to separate large particles from the sample flow. Particles with sufficient inertia are unable to follow the streamlines and are impacted on the impactor plate (Figure 3). If the jet velocity is lower

than intended, the particle Stokes number (eq. 2) will be low too, which means the particle can make the turn through the impactor well and escape from the impaction plate. For example, in an ideal situation, the sampling effectiveness for 4 μm particles would be 0.00%, which means that all of the particles hit the impaction plate and are prevented from reaching the sampler filter. However, in the full wind tests, about 25% of 4 μm particles penetrated the impaction well and were collected by the filter (Table 8). The effectiveness of the impactor for 4μm particles could be decreased by increasing the jet velocity through each nozzle.

In order to test whether low velocity was the reason for the high sampling effectiveness of large particles, the flow rate of sampler was increased from 40 CFM (1133 L/min) to 44 CFM (1246 L/min), and accordingly, the velocity inside the nozzle was raised by 10%. For tests carried out at 2 km/hr wind speed, the sampling effectiveness for 4 μm particles decreased from 22.9% to 5.6% when the sampling flow rate was increased from 40 CFM (1133 L/min) to 44 CFM (1246 L/min), indicating that the low velocity was the cause of high sampling efficiency at large particle.

To correct this problem, Tisch Environmental could redesign the nozzle rack to increase the velocity (i.e. reducing the cross sectional area of each nozzle) in order to comply with the performance metrics of a Class II FEM $PM_{2.5}$ sampler as described in 40 CFR Part 53, Subpart F.

REFERENCES

Berglund, R. N., and B. Y. H. Liu. 1973. Generation of Monodisperse Aerosol Standards. *Environmental Science & Technology* 7(2):147-153.

Brunekreef, B., and S. T. Holgate. 2002. Air pollution and health. *The Lancet* 360(9341):1233-1242.

Faulkner, W. B. 2013. Request for Waiver from 40 CFR 53 Subpart F Tests for Class II PM2.5 FEM Sampler Designation Tisch Environmental High Volume PM2.5 Sampler (approved by EPA).

Faulkner, W. B., and J. S. Haglund. 2012. Flattening Coefficients for Oleic Acid Droplets on Treated Glass Slides. *Aerosol Science and Technology* 46(7):828-832.

Han, T., J. S. Haglund, S. Hari, and A. R. McFarland. 2009. Aerosol deposition on electroformed wire screens. *Aerosol Science and Technology* 43(2):112-119.

Hinds, W. C. 1999. *Aerosol technology: properties, behavior, and measurement of airborne particles*. Wiley (New York).

McMurry, P. H., M. F. Shepherd, J. S. Vickery, and NARSTO. 2004. *Particulate Matter Science for Policy Makers: A NARSTO Assessment*. Cambridge University Press (New York).

Pope III, C. A., R. T. Burnett, M. J. Thun, E. E. Calle, D. Krewski, K. Ito, and G. D. Thurston. 2002. Lung cancer, cardiopulmonary mortality, and long-term exposure to fine particulate air pollution. *JAMA: the Journal of the American Medical Association* 287(9):1132-1141.

USEPA. 1998. PM2.5 Mass Weighing Laboratory Standard Operating Procedures for the Performance Evaluation Program. Available at: http://www.epa.gov/region4/sesd/pm25/p5.html.

USEPA. 2013a. National ambient air quality standards. Available at: http://www.epa.gov/air/criteria.html.

USEPA. 2013b. PM2.5. Available at: http://www.epa.gov/pm/graphics/pm2_5_graphic_lg.jpg.

USEPA. 2013c. Procedures for Testing Performance Characteristics of Class II Equivalent Methods for PM 2.5. CFR40, Part 53, Subpart F. College Park, Maryland.

USEPA. 2013d. Table F-4 to Subpart F of Part 53—Estimated Mass Concentration Measurement of PM2.5 for Idealized Coarse Aerosol Size Distribution. CFR40, Part 53, Subpart F. College Park, Maryland.

APPENDIX A

EFFECTS OF WIRE SCREENS ON THE PERFORMANCE OF TISCH HIGH VOLUME PM2.5 SAMPLER

Wire screens are usually an integral component of an air sampling inlet, it keeps the debris (such as bugs, leafs) out of the sampler. However, it can cause inadvertent deposition of larger aerosol particles. Therefore, it is necessary to find out effects of wire screens on the performance of Tisch Environment high volume PM2.5 sampler inlet.

A correlation form (Han et al., 2009) of the standardized screen efficiency for the electroformed screens can be expressed as:

$$\eta_{ss} = \left[-0.714 + \frac{1.777}{1+0.464\left(\frac{Stk_{0.5}}{Stk}\right)^{0.852}}\right]\left[(1+R)^{0.1}\left(1-\frac{0.03}{Re_w^{0.01}}\right)\right] \quad (1)$$

Where,

η_{ss} is the standardized screen efficiency,

R is the interception parameter=Dp/dw, Dp is the particle diameter and dw is wire width,

Stk is Stokes number,

$Stk_{0.5}$ is Stokes number for which the standardized collection efficiency is 50%,

Re_w is Wire Reynolds number base on average velocity in screen openings.

Figure A-1 shown the correlation curve based on Equation (1) together with the data points upon which the curve is based.

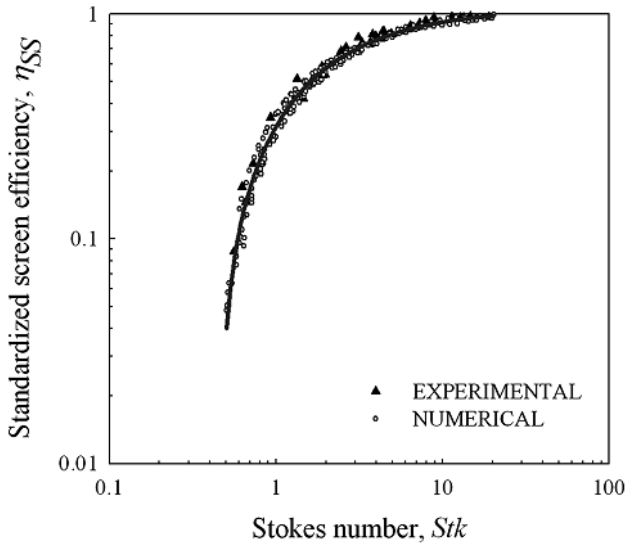

Figure A-1.Correlation curve for standardized efficiency predictions for electroformed wires together with experimental and numerical data

Operation parameters for Tisch high volume PM2.5 sampler

- Diameter of the wire screen: 21.7”,
- Flow rate: 40 CFM,
- Diameter of wire : 60 um,
- Fraction of open area: 0.9.

Table A-1. Stk number for different particle size.

Particle size(um)	1.5	2	2.2	2.5	2.8	3	3.5	4
Stk	0.01	0.03	0.03	0.04	0.05	0.06	0.08	0.10

Based on this parameter, the Stk number can be obtained for each particle size as shown in Table A-1. For all particle sizes, the largest Stk number is 0.1, from Figure , the standardized screen efficiency was less than 0.01. Based on this low efficiency, it can

be assumed that all of the particles pass through the wire screens; the effects of wire screens on the performance of Tisch high volume $PM_{2.5}$ sampler can be ignored.

APPENDIX B

AERODYNAMIC PARTICLE SIZER DATA

Table B-1 Aerodynamic particle sizer data at wind speed of 2km/hr

	1.5um	2um	2.2um	2.5um	2.8um	3.5um	4um
APS AD (um)	**%dM[a]**	**%dM**	**%dM**	**%dM**	**%dM**	**%dM**	**%dM**
<0.523	0.12949	0.052303	0.009261	0.001679	0.001906	0.009042	0.018968
0.542	0.001581	0.001151	0.000942	0.000607	0.000321	0.001667	0.005379
0.583	0.001215	0.001143	0.000877	0.000797	0.000299	0.001379	0.006458
0.626	0.004058	0.001773	0.000943	0.00099	0.000495	0.002567	0.008103
0.673	0.005036	0.002493	0.001081	0.001023	0.000269	0.002549	0.009944
0.723	0.01357	0.003094	0.001453	0.001185	0.000476	0.002109	0.012201
0.777	0.048081	0.002259	0.001109	0.001261	0.000532	0.002944	0.013593
0.835	0.211166	0.001962	0.001893	0.001434	0.000587	0.004871	0.013451
0.898	0.660227	0.002435	0.005125	0.001132	0.000273	0.003022	0.019872
0.965	2.07091	0.002158	0.00318	0.001004	0.000678	0.008125	0.023673
1.037	5.23588	0.00857	0.006248	0.001495	0.001122	0.008532	0.028561
1.114	10.9044	0.014622	0.014282	0.001237	0.000348	0.012513	0.024303
1.197	19.0475	0.046188	0.032409	0.003069	0.001295	0.007166	0.031416
1.286	26.0083	0.158643	0.083577	0.003808	0.002947	0.014822	0.035086
1.382	15.8875	0.440727	0.215226	0.002954	0.003325	0.02575	0.033864
1.486	4.28604	1.58085	0.652221	0.000733	0.011553	0.052497	0.038422

1.596	1.98588	5.35713	2.08105	0.002729	0.02969 6	0.13312 2	0.05214 9
1.715	3.40724	15.1913	6.84582	0.00564 5	0.08958 6	0.22494 9	0.08690 1
1.843	4.96684	31.1039	20.6833	0.08405 4	0.24993 7	0.70223	0.12619 4
1.981	3.34027	27.5721	33.758	1.00829	1.10756	2.13255	0.27048 8
2.129	1.1375	11.9524	20.5827	8.08119	5.3131	5.89051	0.71018 4
2.288	0.32183 8	4.24763	8.91916	38.0463	20.1985	12.6941	1.79328
2.458	0.06306	1.44275	3.91594	38.6921	37.9436	16.9835	4.97847
2.642	0.03477 9	0.51406 5	1.41484	8.59948	21.856	13.7594	14.0439
2.839	0.01079	0.17597 9	0.55373 1	3.00293	8.43028	9.03101	24.6584
3.051	0.05355 8	0.05459 5	0.18435 6	1.79022	3.35138	5.77147	25.3281
3.278	0.03323 1	0.06774 9	0.03119 7	0.58296 1	1.01533	4.3659	14.2315
3.523	0	0	0	0.04888	0.30811 2	2.22191	6.53258
3.786	0.05117 3	0	0	0.01213 1	0.06144 9	1.13312	2.82139
4.068	0	0	0	0	0.00847 3	0.70306 4	1.20815
4.371	0.07880 3	0	0	0.01868 1	0.01051 4	0.17449 2	0.55074 1
4.698	0	0	0	0	0	0.14435 6	0
5.048	0	0	0	0	0	0	0.04711 7
5.425	0	0	0	0	0	0.22229 7	0
5.829	0	0	0	0	0	0	0.14511 2
6.264	0	0	0	0	0	0	0
6.732	0	0	0	0	0	0	0.11173 1
7.234	0	0	0	0	0	0.52714 9	0
7.774	0	0	0	0	0	0	0

8.354	0	0	0	0	0	0	0
8.977	0	0	0	0	0	0	0
9.647	0	0	0	0	0	0	0
10.37	0	0	0	0	0	0	0
11.14	0	0	0	0	0	0	0
11.97	0	0	0	0	0	1.19441	0
12.86	0	0	0	0	0	0	0.779695
13.82	0	0	0	0	0	0	0
14.86	0	0	0	0	0	2.28246	1.20067
15.96	0	0	0	0	0	0	0
17.15	0	0	0	0	0	0	0
18.43	0	0	0	0	0	8.72335	0
19.81	0	0	0	0	0	10.8251	0

[a]%dM means mass percentage

Table B-2 Aerodynamic particle sizer data at wind speed of 24km/hr

	1.5um	2um	2.2um	2.5um	2.8um	3.5um	4um
APS AD (um)	**%dM**	**%dM**	**%dM**	**%dM**	**%dM**	**%dM**	**%dM**
<0.523	0.304526	0.123331	0.083071	0.015592	0.034171	0.095949	0.075505
0.542	0.013453	0.016408	0.001463	0.001454	0.004513	0.014785	0.011175
0.583	0.01646	0.023122	0.002825	0.001805	0.006779	0.019851	0.014597
0.626	0.021593	0.028407	0.002254	0.001723	0.008998	0.023514	0.018416
0.673	0.039106	0.033303	0.002641	0.001853	0.008261	0.028022	0.018733
0.723	0.060211	0.044185	0.002314	0.002741	0.010814	0.035061	0.023943
0.777	0.169509	0.050739	0.00311	0.002744	0.011463	0.037089	0.026539
0.835	0.550095	0.069734	0.00475	0.002315	0.012837	0.047353	0.032217
0.898	1.71989	0.106279	0.003684	0.002873	0.017652	0.062606	0.043533
0.965	5.12312	0.185057	0.00823	0.002307	0.021103	0.065424	0.051817
1.037	11.0251	0.37713	0.00851	0.00338	0.01558	0.07865	0.04993

		5		3			7
1.114	20.2006	0.904694	0.014081	0.007428	0.023448	0.083957	0.066213
1.197	25.8842	2.26327	0.043684	0.01082	0.019909	0.089859	0.070578
1.286	14.2284	5.54917	0.11926	0.035806	0.027239	0.11959	0.069282
1.382	4.35221	12.9624	0.413039	0.085781	0.027513	0.134366	0.07462
1.486	2.26461	21.8382	1.44918	0.270333	0.034142	0.241399	0.088572
1.596	2.96475	20.3391	5.08633	0.950331	0.060527	0.352062	0.079937
1.715	3.72701	13.6164	14.4748	3.65584	0.345504	0.640001	0.133295
1.843	2.22327	8.71231	26.752	11.93	2.4271	1.36013	0.146177
1.981	1.30104	5.7962	27.9358	27.2115	13.4401	3.06879	0.30551
2.129	0.744276	3.48432	14.7146	30.8133	31.1721	7.25751	0.687153
2.288	0.55416	1.59884	5.32252	14.9616	25.1567	14.3953	1.96271
2.458	0.370288	0.871263	1.58125	6.17031	11.2105	21.8559	7.18823
2.642	0.175049	0.353258	0.309825	2.60974	9.95092	19.3267	20.6816
2.839	0.407297	0.26568	0.104857	0.908498	3.94824	12.7992	27.1536
3.051	0.235868	0.2143	0.043374	0.245373	1.23333	5.40926	18.8265
3.278	0.250883	0.061369	0	0.074066	0.503173	2.56735	7.7875
3.523	0.103777	0	0.044528	0.020425	0.117076	1.26109	3.99974
3.786	0.321951	0.063003	0	0	0.064571	0.453009	2.09863
4.068	0.079904	0	0	0	0	0.306631	0.785415
4.371	0.198313	0.04851	0.042545	0	0	0.190255	0.359082
4.698	0.36914	0	0	0	0	0.078698	0.127314
5.048	0	0	0	0	0.03828	0.097659	0.236983

5.425	0	0	0	0	0.047504	0	0.098027
5.829	0	0	0	0	0	0.150388	0.121645
6.264	0	0	0	0	0	0.373245	0.150954
6.732	0	0	0	0	0	0.694761	0.37465
7.234	0	0	0.192798	0	0	0.57477	0
7.774	0	0	0	0	0	0	0.288467
8.354	0	0	0.296895	0	0	0	0.715938
8.977	0	0	0.368428	0	0	0	0.444218
9.647	0	0	0	0	0	1.36299	0
10.37	0	0	0.567352	0	0	0.845696	0
11.14	0	0	0	0	0	2.09891	0
11.97	0	0	0	0	0	1.30231	0
12.86	0	0	0	0	0	0	0
13.82	0	0	0	0	0	0	0
14.86	0	0	0	0	0	0	2.01301
15.96	0	0	0	0	0	0	2.49802
17.15	0	0	0	0	0	0	0
18.43	0	0	0	0	0	0	0
19.81	0	0	0	0	0	0	0

APPENDIX C

ESTIMATED MASS CONCENTRATION MEASUREMENT OF PM2.5 FOR IDEALIZED COARSE AEROSOL SIZE DISTRIBUTION AT WIND SPEED OF 2KM/HR

	Test Sampler			Ideal Sampler		
Particle Aerodynamic Diameter (µm)	**Fractional Sampling Effectiveness**	**Interval Mass Concentration ($\mu g/m^3$)**	**Estimated Mass Concentration Measurement ($\mu g/m^3$)**	**Fractional Sampling Effectiveness**	**Interval Mass Concentration ($\mu g/m^3$)**	**Estimated Mass Concentration Measurement ($\mu g/m^3$)**
(1)	(2)	(3)	(4)	(5)	(6)	(7)
<0.500	1	6.001	6.001	1	6.001	6.001
0.625	1.000	2.129	2.129	0.999	2.129	2.127
0.75	1.000	0.982	0.982	0.998	0.982	0.98
0.875	0.999	0.73	0.729	0.997	0.73	0.728
1	0.997	0.551	0.549	0.995	0.551	0.548
1.125	0.993	0.428	0.425	0.991	0.428	0.424
1.25	0.987	0.346	0.341	0.987	0.346	0.342
1.375	0.976	0.294	0.287	0.98	0.294	0.288
1.5	0.960	0.264	0.254	0.969	0.264	0.256
1.675	0.930	0.251	0.234	0.954	0.251	0.239
1.75	0.914	0.25	0.229	0.932	0.25	0.233
1.875	0.884	0.258	0.228	0.899	0.258	0.232
2	0.849	0.272	0.231	0.854	0.272	0.232
2.125	0.810	0.292	0.237	0.791	0.292	0.231
2.25	0.769	0.314	0.241	0.707	0.314	0.222
2.375	0.726	0.339	0.246	0.602	0.339	0.204
2.5	0.681	0.366	0.249	0.48	0.366	0.176
2.625	0.636	0.394	0.251	0.351	0.394	0.138
2.75	0.591	0.422	0.249	0.23	0.422	0.097

2.875	0.547	0.449	0.246	0.133	0.449	0.06
3	0.505	0.477	0.241	0.067	0.477	0.032
3.125	0.464	0.504	0.234	0.03	0.504	0.015
3.25	0.425	0.53	0.225	0.012	0.53	0.006
3.375	0.388	0.555	0.215	0.004	0.555	0.002
3.5	0.353	0.579	0.205	0.001	0.579	0.001
3.625	0.321	0.602	0.193	0	0.602	0
3.75	0.291	0.624	0.182	0	0.624	0
3.875	0.264	0.644	0.170	0	0.644	0
4	0.238	0.663	0.158	0	0.663	0
4.125	0.215	0.681	0.146	0	0.681	0
4.25	0.193	0.697	0.135	0	0.697	0
4.375	0.174	0.712	0.124	0	0.712	0
4.5	0.156	0.726	0.114	0	0.726	0
4.625	0.141	0.738	0.104	0	0.738	0
4.75	0.126	0.75	0.095	0	0.75	0
4.875	0.113	0.76	0.086	0	0.76	0
5	0.101	0.769	0.078	0	0.769	0
5.125	0.091	0.777	0.070	0	0.777	0
5.25	0.081	0.783	0.064	0	0.783	0
5.375	0.073	0.789	0.057	0	0.789	0
5.5	0.065	0.794	0.052	0	0.794	0
5.625	0.058	0.798	0.046	0	0.798	0
5.75	0.052	0.801	0.042	0	0.801	0
		$C_{sam(exp)}$=	17.372		$C_{ideal(exp)}$=	13.814

APPENDIX D

ESTIMATED MASS CONCENTRATION MEASUREMENT OF PM2.5 FOR IDEALIZED COARSE AEROSOL SIZE DISTRIBUTION AT WIND SPEED OF 24KM/HR

	Test Sampler			**Ideal Sampler**		
Particle Aerodynamic Diameter (μm)	**Fractional Sampling Effectiveness**	**Interval Mass Concentration ($\mu g/m^3$)**	**Estimated Mass Concentration Measurement ($\mu g/m^3$)**	**Fractional Sampling Effectiveness**	**Interval Mass Concentration ($\mu g/m^3$)**	**Estimated Mass Concentration Measurement ($\mu g/m^3$)**
(1)	(2)	(3)	(4)	(5)	(6)	(7)
<0.500	1	6.001	6.001	1	6.001	6.001
0.625	1.000	2.129	2.129	0.999	2.129	2.127
0.75	1.000	0.982	0.982	0.998	0.982	0.98
0.875	0.999	0.73	0.729	0.997	0.73	0.728
1	0.997	0.551	0.549	0.995	0.551	0.548
1.125	0.993	0.428	0.425	0.991	0.428	0.424
1.25	0.987	0.346	0.341	0.987	0.346	0.342
1.375	0.976	0.294	0.287	0.98	0.294	0.288
1.5	0.960	0.264	0.254	0.969	0.264	0.256
1.675	0.930	0.251	0.234	0.954	0.251	0.239
1.75	0.914	0.25	0.229	0.932	0.25	0.233
1.875	0.884	0.258	0.228	0.899	0.258	0.232
2	0.849	0.272	0.231	0.854	0.272	0.232
2.125	0.810	0.292	0.237	0.791	0.292	0.231
2.25	0.769	0.314	0.241	0.707	0.314	0.222
2.375	0.726	0.339	0.246	0.602	0.339	0.204
2.5	0.681	0.366	0.249	0.48	0.366	0.176
2.625	0.636	0.394	0.251	0.351	0.394	0.138
2.75	0.591	0.422	0.249	0.23	0.422	0.097

2.875	0.547	0.449	0.246	0.133	0.449	0.06
3	0.505	0.477	0.241	0.067	0.477	0.032
3.125	0.464	0.504	0.234	0.03	0.504	0.015
3.25	0.425	0.53	0.225	0.012	0.53	0.006
3.375	0.388	0.555	0.215	0.004	0.555	0.002
3.5	0.353	0.579	0.205	0.001	0.579	0.001
3.625	0.321	0.602	0.193	0	0.602	0
3.75	0.291	0.624	0.182	0	0.624	0
3.875	0.264	0.644	0.170	0	0.644	0
4	0.238	0.663	0.158	0	0.663	0
4.125	0.215	0.681	0.146	0	0.681	0
4.25	0.193	0.697	0.135	0	0.697	0
4.375	0.174	0.712	0.124	0	0.712	0
4.5	0.156	0.726	0.114	0	0.726	0
4.625	0.141	0.738	0.104	0	0.738	0
4.75	0.126	0.75	0.095	0	0.75	0
4.875	0.113	0.76	0.086	0	0.76	0
5	0.101	0.769	0.078	0	0.769	0
5.125	0.091	0.777	0.070	0	0.777	0
5.25	0.081	0.783	0.064	0	0.783	0
5.375	0.073	0.789	0.057	0	0.789	0
5.5	0.065	0.794	0.052	0	0.794	0
5.625	0.058	0.798	0.046	0	0.798	0
5.75	0.052	0.801	0.042	0	0.801	0
		$C_{sam(exp)}$=	17.372		$C_{ideal(exp)}$=	13.814

APPENDIX E

ESTIMATED MASS CONCENTRATION MEASUREMENT OF PM2.5 FOR IDEALIZED "TYPICAL" COARSE AEROSOL SIZE DISTRIBUTION AT WIND SPEED OF 2 KM/HR

	Test Sampler			**Ideal Sampler**		
Particle Aerodynamic Diameter (µm)	**Fractional Sampling Effectiveness**	**Interval Mass Concentration ($\mu g/m^3$)**	**Estimated Mass Concentration Measurement ($\mu g/m^3$)**	**Fractional Sampling Effectiveness**	**Interval Mass Concentration ($\mu g/m^3$)**	**Estimated Mass Concentration Measurement ($\mu g/m^3$)**
(1)	(2)	(3)	(4)	(5)	(6)	(7)
<0.500	1	16.651	16.651	1	16.651	16.651
0.625	0.99996	5.899	5.899	0.999	5.899	5.893
0.75	0.99977	2.708	2.707	0.998	2.708	2.703
0.875	0.99907	1.996	1.994	0.997	1.996	1.99
1	0.99726	1.478	1.474	0.995	1.478	1.471
1.125	0.99344	1.108	1.101	0.991	1.108	1.098
1.25	0.98663	0.846	0.835	0.987	0.846	0.835
1.375	0.97589	0.661	0.645	0.98	0.661	0.648
1.5	0.96049	0.532	0.511	0.969	0.532	0.516
1.675	0.93039	0.444	0.413	0.954	0.444	0.424
1.75	0.91441	0.384	0.351	0.932	0.384	0.358
1.875	0.88391	0.347	0.307	0.899	0.347	0.312
2	0.84903	0.325	0.276	0.854	0.325	0.277
2.125	0.81048	0.314	0.254	0.791	0.314	0.248
2.25	0.76908	0.312	0.240	0.707	0.312	0.221
2.375	0.72565	0.316	0.229	0.602	0.316	0.19
2.5	0.68103	0.325	0.221	0.48	0.325	0.156
2.625	0.636	0.336	0.214	0.351	0.336	0.118
2.75	0.59122	0.35	0.207	0.23	0.35	0.081

2.875	0.54727	0.366	0.200	0.133	0.366	0.049
3	0.50465	0.382	0.193	0.067	0.382	0.026
3.125	0.4637	0.399	0.185	0.03	0.399	0.012
3.25	0.42472	0.416	0.177	0.012	0.416	0.005
3.375	0.38788	0.432	0.168	0.004	0.432	0.002
3.5	0.35332	0.449	0.159	0.001	0.449	0
3.625	0.32107	0.464	0.149	0	0.464	0
3.75	0.29114	0.48	0.140	0	0.48	0
3.875	0.2635	0.494	0.130	0	0.494	0
4	0.23807	0.507	0.121	0	0.507	0
4.125	0.21477	0.52	0.112	0	0.52	0
4.25	0.19349	0.532	0.103	0	0.532	0
4.375	0.1741	0.543	0.095	0	0.543	0
4.5	0.15649	0.553	0.087	0	0.553	0
4.625	0.14053	0.562	0.079	0	0.562	0
4.75	0.12609	0.57	0.072	0	0.57	0
4.875	0.11305	0.577	0.065	0	0.577	0
5	0.10129	0.584	0.059	0	0.584	0
5.125	0.09072	0.59	0.054	0	0.59	0
5.25	0.0812	0.595	0.048	0	0.595	0
5.375	0.07266	0.599	0.044	0	0.599	0
5.5	0.065	0.603	0.039	0	0.603	0
5.625	0.05813	0.605	0.035	0	0.605	0
5.75	0.05197	0.608	0.032	0	0.608	0
		$C_{sam(exp)}$=	37.072		$C_{ideal(exp)}$=	34.284

APPENDIX F

ESTIMATED MASS CONCENTRATION MEASUREMENT OF PM2.5 FOR IDEALIZED "TYPICAL" COARSE AEROSOL SIZE DISTRIBUTION AT WIND SPEED OF 24 KM/HR

	Test Sampler			**Ideal Sampler**		
Particle Aerodynamic Diameter (µm)	**Fractional Sampling Effectiveness**	**Interval Mass Concentration ($\mu g/m^3$)**	**Estimated Mass Concentration Measurement ($\mu g/m^3$)**	**Fractional Sampling Effectiveness**	**Interval Mass Concentration ($\mu g/m^3$)**	**Estimated Mass Concentration Measurement ($\mu g/m^3$)**
(1)	(2)	(3)	(4)	(5)	(6)	(7)
<0.500	1	16.651	16.651	1	16.651	16.651
0.625	1	5.899	5.899	0.999	5.899	5.893
0.75	0.99999	2.708	2.708	0.998	2.708	2.703
0.875	0.99994	1.996	1.996	0.997	1.996	1.99
1	0.99974	1.478	1.478	0.995	1.478	1.471
1.125	0.99909	1.108	1.107	0.991	1.108	1.098
1.25	0.99746	0.846	0.844	0.987	0.846	0.835
1.375	0.99409	0.661	0.657	0.98	0.661	0.648
1.5	0.98802	0.532	0.526	0.969	0.532	0.516
1.675	0.97308	0.444	0.432	0.954	0.444	0.424
1.75	0.96386	0.384	0.370	0.932	0.384	0.358
1.875	0.94424	0.347	0.328	0.899	0.347	0.312
2	0.91904	0.325	0.299	0.854	0.325	0.277
2.125	0.88831	0.314	0.279	0.791	0.314	0.248
2.25	0.85243	0.312	0.266	0.707	0.312	0.221
2.375	0.81205	0.316	0.257	0.602	0.316	0.19
2.5	0.76801	0.325	0.250	0.48	0.325	0.156
2.625	0.72127	0.336	0.242	0.351	0.336	0.118
2.75	0.67282	0.35	0.235	0.23	0.35	0.081

2.875	0.62361	0.366	0.228	0.133	0.366	0.049
3	0.57452	0.382	0.219	0.067	0.382	0.026
3.125	0.52631	0.399	0.210	0.03	0.399	0.012
3.25	0.47961	0.416	0.200	0.012	0.416	0.005
3.375	0.43494	0.432	0.188	0.004	0.432	0.002
3.5	0.39265	0.449	0.176	0.001	0.449	0
3.625	0.35301	0.464	0.164	0	0.464	0
3.75	0.31617	0.48	0.152	0	0.48	0
3.875	0.28219	0.494	0.139	0	0.494	0
4	0.25106	0.507	0.127	0	0.507	0
4.125	0.22272	0.52	0.116	0	0.52	0
4.25	0.19706	0.532	0.105	0	0.532	0
4.375	0.17393	0.543	0.094	0	0.543	0
4.5	0.15319	0.553	0.085	0	0.553	0
4.625	0.13465	0.562	0.076	0	0.562	0
4.75	0.11815	0.57	0.067	0	0.57	0
4.875	0.1035	0.577	0.060	0	0.577	0
5	0.09053	0.584	0.053	0	0.584	0
5.125	0.07909	0.59	0.047	0	0.59	0
5.25	0.06902	0.595	0.041	0	0.595	0
5.375	0.06016	0.599	0.036	0	0.599	0
5.5	0.05239	0.603	0.032	0	0.603	0
5.625	0.04559	0.605	0.028	0	0.605	0
5.75	0.03965	0.608	0.024	0	0.608	0
		$C_{sam(exp)}$=	37.489		$C_{ideal(exp)}$=	34.284

APPENDIX G

ESTIMATED MASS CONCENTRATION MEASUREMENT OF PM2.5 FOR IDEALIZED FINE AEROSOL SIZE DISTRIBUTION AT WIND SPEED OF 2KM/HR

	Test Sampler			Ideal Sampler		
Particle Aerodynamic Diameter (µm)	**Fractional Sampling Effectiveness**	**Interval Mass Concentration ($\mu g/m^3$)**	**Estimated Mass Concentration Measurement ($\mu g/m^3$)**	**Fractional Sampling Effectiveness**	**Interval Mass Concentration ($\mu g/m^3$)**	**Estimated Mass Concentration Measurement ($\mu g/m^3$)**
(1)	(2)	(3)	(4)	(5)	(6)	(7)
<0.500	1	18.868	18.868	1	18.868	18.868
0.625	0.99996	13.412	13.411	0.999	13.412	13.399
0.75	0.99977	8.014	8.012	0.998	8.014	7.998
0.875	0.99907	6.984	6.978	0.997	6.984	6.963
1	0.99726	5.954	5.938	0.995	5.954	5.924
1.125	0.99344	5.015	4.982	0.991	5.015	4.97
1.25	0.98663	4.197	4.141	0.987	4.197	4.142
1.375	0.97589	3.503	3.419	0.98	3.503	3.433
1.5	0.96049	2.921	2.806	0.969	2.921	2.83
1.675	0.93039	2.438	2.268	0.954	2.438	2.326
1.75	0.91441	2.039	1.864	0.932	2.039	1.9
1.875	0.88391	1.709	1.511	0.899	1.709	1.536
2	0.84903	1.437	1.220	0.854	1.437	1.227
2.125	0.81048	1.212	0.982	0.791	1.212	0.959
2.25	0.76908	1.026	0.789	0.707	1.026	0.725
2.375	0.72565	0.873	0.633	0.602	0.873	0.526
2.5	0.68103	0.745	0.507	0.48	0.745	0.358
2.625	0.636	0.638	0.406	0.351	0.638	0.224
2.75	0.59122	0.55	0.325	0.23	0.55	0.127
2.875	0.54727	0.476	0.261	0.133	0.476	0.063
3	0.50465	0.414	0.209	0.067	0.414	0.028

3.125	0.4637	0.362	0.168	0.03	0.362	0.011
3.25	0.42472	0.319	0.135	0.012	0.319	0.004
3.375	0.38788	0.282	0.109	0.004	0.282	0.001
3.5	0.35332	0.252	0.089	0.001	0.252	0
3.625	0.32107	0.226	0.073	0	0.226	0
3.75	0.29114	0.204	0.059	0	0.204	0
3.875	0.2635	0.185	0.049	0	0.185	0
4	0.23807	0.17	0.040	0	0.17	0
4.125	0.21477	0.157	0.034	0	0.157	0
4.25	0.19349	0.146	0.028	0	0.146	0
4.375	0.1741	0.136	0.024	0	0.136	0
4.5	0.15649	0.129	0.020	0	0.129	0
4.625	0.14053	0.122	0.017	0	0.122	0
4.75	0.12609	0.117	0.015	0	0.117	0
4.875	0.11305	0.112	0.013	0	0.112	0
5	0.10129	0.108	0.011	0	0.108	0
5.125	0.09072	0.105	0.010	0	0.105	0
5.25	0.0812	0.102	0.008	0	0.102	0
5.375	0.07266	0.1	0.007	0	0.1	0
5.5	0.065	0.098	0.006	0	0.098	0
5.625	0.05813	0.097	0.006	0	0.097	0
5.75	0.05197	0.096	0.005	0	0.096	0
		$C_{sam(exp)}$=	80.456		$C_{ideal(exp)}$=	78.539

APPENDIX H

ESTIMATED MASS CONCENTRATION MEASUREMENT OF PM2.5 FOR IDEALIZED FINE AEROSOL SIZE DISTRIBUTION AT WIND SPEED OF 24KM/HR

	Test Sampler			**Ideal Sampler**		
Particle Aerodynamic Diameter (µm)	**Fractional Sampling Effectiveness**	**Interval Mass Concentration ($\mu g/m^3$)**	**Estimated Mass Concentration Measurement ($\mu g/m^3$)**	**Fractional Sampling Effectiveness**	**Interval Mass Concentration ($\mu g/m^3$)**	**Estimated Mass Concentration Measurement ($\mu g/m^3$)**
(1)	(2)	(3)	(4)	(5)	(6)	(7)
<0.500	1	18.868	18.868	1	18.868	18.868
0.625	1	13.412	13.412	0.999	13.412	13.399
0.75	0.99999	8.014	8.014	0.998	8.014	7.998
0.875	0.99994	6.984	6.984	0.997	6.984	6.963
1	0.99974	5.954	5.952	0.995	5.954	5.924
1.125	0.99909	5.015	5.010	0.991	5.015	4.97
1.25	0.99746	4.197	4.186	0.987	4.197	4.142
1.375	0.99409	3.503	3.482	0.98	3.503	3.433
1.5	0.98802	2.921	2.886	0.969	2.921	2.83
1.675	0.97308	2.438	2.372	0.954	2.438	2.326
1.75	0.96386	2.039	1.965	0.932	2.039	1.9
1.875	0.94424	1.709	1.614	0.899	1.709	1.536
2	0.91904	1.437	1.321	0.854	1.437	1.227
2.125	0.88831	1.212	1.077	0.791	1.212	0.959
2.25	0.85243	1.026	0.875	0.707	1.026	0.725
2.375	0.81205	0.873	0.709	0.602	0.873	0.526
2.5	0.76801	0.745	0.572	0.48	0.745	0.358
2.625	0.72127	0.638	0.460	0.351	0.638	0.224
2.75	0.67282	0.55	0.370	0.23	0.55	0.127

2.875	0.62361	0.476	0.297	0.133	0.476	0.063
3	0.57452	0.414	0.238	0.067	0.414	0.028
3.125	0.52631	0.362	0.191	0.03	0.362	0.011
3.25	0.47961	0.319	0.153	0.012	0.319	0.004
3.375	0.43494	0.282	0.123	0.004	0.282	0.001
3.5	0.39265	0.252	0.099	0.001	0.252	0
3.625	0.35301	0.226	0.080	0	0.226	0
3.75	0.31617	0.204	0.064	0	0.204	0
3.875	0.28219	0.185	0.052	0	0.185	0
4	0.25106	0.17	0.043	0	0.17	0
4.125	0.22272	0.157	0.035	0	0.157	0
4.25	0.19706	0.146	0.029	0	0.146	0
4.375	0.17393	0.136	0.024	0	0.136	0
4.5	0.15319	0.129	0.020	0	0.129	0
4.625	0.13465	0.122	0.016	0	0.122	0
4.75	0.11815	0.117	0.014	0	0.117	0
4.875	0.1035	0.112	0.012	0	0.112	0
5	0.09053	0.108	0.010	0	0.108	0
5.125	0.07909	0.105	0.008	0	0.105	0
5.25	0.06902	0.102	0.007	0	0.102	0
5.375	0.06016	0.1	0.006	0	0.1	0
5.5	0.05239	0.098	0.005	0	0.098	0
5.625	0.04559	0.097	0.004	0	0.097	0
5.75	0.03965	0.096	0.004	0	0.096	0
		$C_{sam(exp)}$=	81.662		$C_{ideal(exp)}$=	78.539